Published online 25 October 2015

Nucleic Acids Research, 2016, Vol. 44, No. 2 ***695–704***
doi: 10.1093/nar/gkv1109

Recombinational repair of radiation-induced double-strand breaks occurs in the absence of extensive resection

James W. Westmoreland and Michael A. Resnick*

Chromosome Stability Section, Genome Integrity and Structural Biology Laboratory, National Institute of Environmental Health Sciences, NIH, Research Triangle Park, NC 27709, USA

Received April 06, 2015; Revised October 05, 2015; Accepted October 13, 2015

ABSTRACT

Recombinational repair provides accurate chromosomal restitution after double-strand break (DSB) induction. While all DSB recombination repair models include 5′-3′ resection, there are no studies that directly assess the resection needed for repair between sister chromatids in G-2 arrested cells of random, radiation-induced 'dirty' DSBs. Using our Pulse Field Gel Electrophoresis-shift approach, we determined resection at IR-DSBs in WT and mutants lacking exonuclease1 or Sgs1 helicase. Lack of either reduced resection length by half, without decreased DSB repair or survival. In the *exo1Δ sgs1Δ* double mutant, resection was barely detectable, yet it only took an additional hour to achieve a level of repair comparable to WT and there was only a 2-fold dose-modifying effect on survival. Results with a Dnl4 deletion strain showed that remaining repair was not due to end-joining. Thus, similar to what has been shown for a single, clean HO-induced DSB, a severe reduction in resection tract length has only a modest effect on repair of multiple, dirty DSBs in G2-arrested cells. Significantly, this study provides the first opportunity to directly relate resection length at DSBs to the capability for global recombination repair between sister chromatids.

INTRODUCTION

The ability to repair DNA double-strand breaks (DSBs) is a common requirement among all double-strand DNA containing organisms. That said, DSBs arise in many ways. They can be created directly by enzymes, during replication (i.e. fork-collapse) and in response to DNA damaging agents through closely-spaced single-strand breaks, or derived from overlapping processing of nearby single-strand lesions, as well as creation of breaks in single-strand regions. The ends could be complex or 'dirty' as described for radiation damage (1,2) and might even be protein linked. There can be dramatic differences in the impact and processing of various types of DSBs. Even for enzymatically induced DSBs, blunt end breaks are far more lethal than breaks with overlapping complementary ends (3).

There are two general mechanisms for repair of DSBs, one involving recombination to restore accurately the genetic information in the broken region and the other consisting of error-prone endjoining that may involve microhomology associations between the broken ends. Resection of the ends is generally acknowledged to be a crucial determining factor in the choice between the two mechanisms of repair (4,5). In the first (6) and all subsequent models of recombinational repair ((7) and summarized in (8)), the initial processing step involves a 5′ to 3′ excision process that exposes a 3′ single-strand end. Through interactions with various recombination proteins, the 3′ end is then available for strand invasion (or in some cases complementary strand-annealing between resected repeats) followed by a series of events that complete the error-free repair process. In human cells, choices between recombinational repair and end-joining are determined by the opportunities for resection as mediated by 53BP1 and BRCA1 (summarized in (9)) as well as Rif1 (10). Previously, using the pulsed-field gel electrophoresis (PFGE) shift assay, we found that there was little resection of ionizing radiation (IR) induced DSBs in human cells (11).

While resection is generally acknowledged to play a key role in DSB recombinational repair, there have been no studies that directly assess the relationship between amount of resection at so-called dirty DSBs and repair efficiency. The only information that is available has been acquired by characterizing unique enzyme-induced 'clean' DSBs (such as by HO endonuclease or ISceI endonuclease; summarized in (12)). Resection at clean DSBs has been described as a two-step process where the roles of MRX (Mre11/Rad50/Xrs2 in budding yeast; MRN in mammalian cells) and Sae2 (CtIP) are limited to an initial *short* resection step (<50–100 bases) followed by *extensive* re-

*To whom correspondence should be addressed. Tel: +1 919 541 4480; Fax: +1 919 541 4704; Email: resnick@niehs.nih.gov

section carried out by Exo1 and/or the combination of Sgs1/Dna2 which can span thousands of bases (13,14). In the absence of MRX or Sae2, Exo1 or Sgs1/Dna2 can initiate resection, although less efficiently.

We have been especially interested in resection and repair of DSBs produced by IR, a common source of environmental DSBs and one of the most common agents used in cancer treatments. There has been a large void of information connecting the role of various gene products in resecting damaged DNA, their effects on DSB repair and the consequences for cellular survival. Given that the IR-induced DSBs (herein referred to as IR-DSBs) are produced randomly throughout a genome, we developed a novel approach for quantitating resection and relating it to efficiency of DSB repair in budding yeast. Ours is a natural substrate repair system where DSBs are randomly induced in sister chromatids of G2-arrested cells. At any break site there would most likely be an unbroken homolog from which to repair, unlike the situation with enzyme-induced DSBs that cut sister chromatids at the same position, thereby preventing recombinational repair between the chromatids.

Briefly, we have employed circular ChrIII and PFGE to monitor resection at a randomly appearing, radiation-induced single DSB in the circular chromosome (15,16). (A diagram of the resection assay is presented in Supplementary Figure S1.) Intact circular molecules are retained in the starting well. At low doses, molecules that experience a single DSB (regardless of position in the chromosome) would migrate as a population of linear DNAs of unique size and, therefore, would be detectable as a single band, as initially described by Game *et al.* (17). With increased dose, multiple breaks would result in a distribution of linear molecules that run faster than the full length, single DSB band. We found that with time after irradiation of G2 cells, when recombinational repair occurs preferentially between sister chromatids even in diploid cells (18), the singly broken molecules exhibited slower mobilities. This phenomenon, which we had referred to as *PFGE-shift*, was due to resection at the ends of the molecules (described further in the Results; see (15) for possible reasons). Resection occurred at the rate of approximately 1–2 kb per hour at each end and nearly 50% of the IR-DSBs across the genome were repaired within a half-hour based on increases in the amounts of restored chromosomes. The PFGE-shift was also used to quantify the appearance of derived DSBs following treatment with the single-strand damaging agent methylmethane sulfonate and subsequent resection (19). In addition, we demonstrated for the first time, the induction by IR-DSBs of molecular recombinants between sister chromatids as evidenced by the creation of linear dimer molecules ((15), which also includes a description of how the recombinants may have formed). These dimers were also subject to resection.

Using the PFGE-shift assay, we found (20) that there was coincident initiation of resection at both ends of a DSB, which we proposed was due to a coordination of resection between the ends. The coordination at IR-DSBs required Sae2 in budding yeast (Ctp1 fission yeast; CtIP mammalian), the Mre11/Rad50/Xrs2 complex (MRX budding yeast; MRN mammalian) and specifically the Mre11 nuclease. In the absence of Sae2 or Mre11 nuclease, there was limited resection as indicated by partial PFGE-shift, which was proposed to be due to uncoordinated resection at only one end of an IR-DSB. In that study, we found that neither Sae2 nor Mre11 nuclease are required for efficient resection of 'clean' enzymatic DSBs while they were essential for radiation-induced 'dirty' DSBs. These findings provided the first clear distinction between resection requirements and repair of different kinds of DSBs.

Several studies have addressed the impact of altering reducing resection length at a single, clean DSB on various types of recombination (cf., (14,21,22)). A substantial reduction in length of resection had a modest effect on recombination. Since both chromatids would be cut in these systems, it would not be possible to address sister chromatid recombination. However, a plasmid-based system has been developed to address sister chromatid repair of a DSB arising during replication (TINV assay; (23)). A partial HO recognition site was created at which an HO endonuclease can create a single-strand nick. During replication this converts to a DSB such that the uncut sister chromatid is available for recombinational repair leading to equal (allelic) or unequal (between repeats) sister chromatid exchange on the plasmid. Equal exchange events (as would be expected between chromosomal sister chromatids) were 3-fold greater than unequal. While these experiments are highly informative, little is known about the impact of reduced resection on recombinational repair between sister chromatids following the induction of multiple dirty DSBs. This is particularly relevant given our previous findings of differences in processing clean versus dirty breaks (20).

Therefore, we set out to modify the levels of resection at IR-DSBs and assess the consequences on their repair by recombination and possibly endjoining, as well as the generation of recombinant molecules as measured by dimer formation. Previously, MRX had been shown to play a role at initiating resection at a defined DSB, followed by further extensive resection by exonuclease 1 (Exo1) or the Sgs1/Dna2 helicase/nuclease combination (24). Loss of the nucleases reduced resection of the single clean break resulting in reduced repair by single-strand annealing of a single clean break placed between direct repeats (14,25). Here, we show that a lack of either Exo1 or Sgs1/Dna2 reduces the rate of resection at IR-DSBs by half, with little if any consequences to DSB repair. The combined loss of Exo1 and Sgs1/Dna2 results in barely detectable levels of resection of IR-DSBs. Yet, there is only a relatively small reduction in the rate of DSB repair or survival, suggesting that in WT cells there is far more resection than is needed for repair or generation of recombinant dimer molecules. Crucially, we demonstrate that the low-resection repair is due to recombination and not endjoining. Our results raise an intriguing possibility that recombinational repair of DSBs in yeast and in vertebrates might be more similar mechanistically than previously realized.

MATERIALS AND METHODS

Strains

The strains used in this study, described in Supplementary Table S1, are haploid and contain a circular ChrIII derived from MWJ49 and MWJ50 (26). All gene deletions were made by replacing the relevant ORFs with the

dominant selectable marker cassettes G418 (*kanMX4*), hygromycin (*hphMX4*) or nourseothricin (*natMX4*), as described in (27). The *mre11-null* construct used in this study was made by replacement of 485 bp of the *MRE11* locus (starting at 215 bases upstream of the start codon) by the KanMX-URA3 core cassette (28) as described in (20).

Nocodazole arrest, gamma irradiation and post-IR incubation

Yeast cells were cultured overnight at 30°C in YPDA media (1% yeast extract, 2% Bacto-Peptone, 2% dextrose, 60 μg/ml adenine sulfate). Nocodazole (United States Biological, Swampscott, MA, USA) was added to the logarithmically growing cells the next morning at a final concentration of 20 micrograms/ml to arrest cells in G2. Cell morphology was checked microscopically to monitor G2 arrest. After 3 to 4 h of nocodazole treatment, the cells were harvested by centrifugation, the pellets were washed and resuspended in ice-cold sterile water at ~5×10^7 cells/ml. Cells were irradiate in a ^{137}Cs irradiator (J. L. Shepherd Model 431); the cell suspensions were kept on ice during the irradiation procedure. The irradiated cells were centrifuged and resuspended in 30°C YPDA containing 20 μg/ml nocodazole for postirradiation incubation.

PFGE procedures

Plugs for PFGE were prepared as described previously (15). PFGE was carried out using a CHEF Mapper XA system (Bio-Rad, Hercules, CA, USA), which was programmed in autoalgorithm mode, 250–1400 kb, 24 h total run time, using $\frac{1}{2}$ X TBE (44.5 mM Tris, 44.5 mM boric acid, 2 mM EDTA) as running buffer. Gels were stained in Sybr® Gold (Invitrogen) and images were photographed and analyzed for quantitation of DSBs using a Kodak GelLogic 200 digital imaging system.

Southern transfer hybridization

Procedures for Southern transfers, preparation of probes, ^{32}P labeling and hybridization were previously described (26).

Quantitation of DSBs

The estimations of DSBs in Figures 3D and 4C were carried out using the previously described 'stained gel, multiple band method' (15), except that in the present study, the data are presented as% DSBs repaired rather than% DSBs remaining. Briefly, PFGE gels were stained with Sybr®Gold and multiple bands that were well-separated were quantitated from each lane and related to corresponding bands in unirradiated control lanes using a Poisson formula to calculate the average number of DSBs per Mb for each sample lane. This method does not require a loading control to compensate for differences in amount of DNA loaded per lane as discussed in (15).

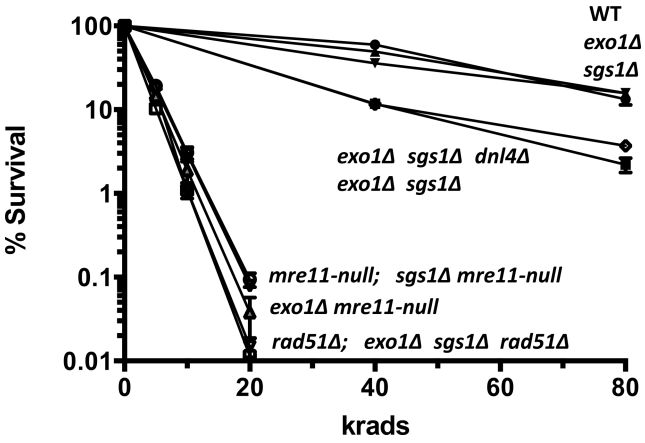

Figure 1. IR-survival in cells lacking extensive resection (*exo1Δsgs1Δ*) is high relative to that in *rad51Δ* or *mre11-null* cells. G2/M nocadazole-arrested cells were irradiated in ice-cold deionized water and appropriate dilutions were plated to YPDA and cells were incubated at 30°C for at least 3 days before counting colonies. Error bars are SEM and all data sets are averages of at least three experiments, except for *exo1Δ*, *sgs1Δ*, *rad51Δ* and *exo1Δ*, *sgs1Δ*, *dnl4Δ*, triple mutants, where there were two experiments. In many cases, the error bars are smaller than the symbols. Key to symbols (in order of increasing IR sensitivity): WT, closed circle; *exo1Δ*, closed triangle; *sgs1Δ*, closed, inverted triangle; *exo1Δ sgs1Δ dnl4Δ*, open diamond; *exo1Δ sgs1Δ*, closed square; *mre11-null*, open circle; *sgs1Δ mre11-null*, gray, inverted triangle; *exo1Δ mre11-null*, gray triangle; *rad51Δ*, open, inverted triangle; *exo1Δ sgs1Δ rad51Δ*, open, inverted square.

RESULTS

Impact of resection deficiency on survival following IR

Unlike DSBs induced by enzymes such as HO or I-SceI, breaks produced by IR and various carcinogens typically have dirty ends that may affect their ability to be processed and repaired, which might impact survival. We have addressed the roles of Exo1 and Sgs1/Dna2 on the ability of haploid G-2 cells to survive IR. Cells at this stage are maximally resistant to IR due to availability of sister chromatids as recombination partners. As shown in Figure 1, the wild type (WT) G2 cells exhibit nearly 20% survival following exposure to 80 krad, corresponding to ~160 DSBs per haploid G2 cell (based on DSB induction estimates from (15,29)). Since the survival appears comparable to or only slightly reduced in the *exo1Δ* and the *sgs1Δ* mutants, but clearly decreased in the double-mutants, they may have redundant functions, in accord with studies on resection of HO-induced DSBs (13,14). However, even for the double mutant there is only a dose-modify factor of 2 compared to WT (this factor, DMF, is the fold increase in dose required to obtain equivalent killing). Thus, the effect of the loss of both DNA resection factors on IR survival is small, especially as compared to *rad51Δ* or *mre11-null* cells, which are severely deficient in DSB recombinational repair.

Loss of either Exo1 or Sgs1 reduces resection at IR-DSBs but not DSB repair

Based on our findings that *exo1Δ* and *sgs1Δ* G-2 cells, like the WT, could tolerate comparable amounts of IR-DSBs and a combined *exo1Δ sgs1Δ* defect has only a modest effect on survival of haploid G-2 cells, we examined the effects

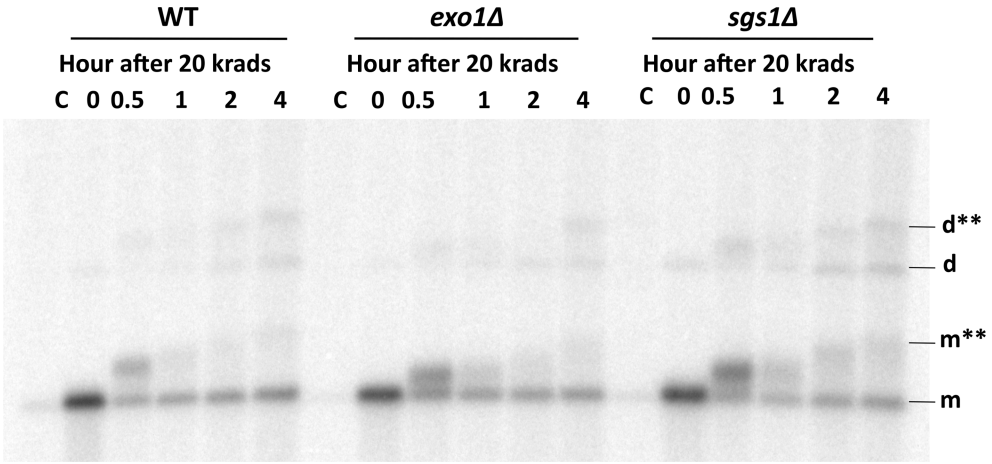

Figure 2. Processive resection is slower in the absence of either Exo1 or Sgs1, but efficient repair reduces detection of PFGE shifted molecules after 1 h. G2/M-arrested cells were irradiated at 20 krads and returned to liquid YPDA to monitor resection/PFGE-shift and DSB repair. 'm' indicates the position of the linearized circular ChrIII monomer before resection and the m** corresponding to PFGE-shift indicates the final shifted position of linearized monomer after extensive resection at both ends of the DSB during 4 h of post-IR incubation in YPDA at 30°C. Likewise, 'd' and 'd**' indicate the positions of recombinant unresected and resected dimers that appear during the postirradiation incubation. The kinetics of resection/PFGE-shift appear reduced in both of the single mutants, but PFGE- shift at later time points was difficult to detect as most linearized molecules recircularized due to DSB repair.

of the mutants on resection of random IR-DSBs. Previous results addressing resection from a 'clean' HO-induced DSB in *exo1Δ* and *sgs1Δ* single mutants have varied with little apparent difference between the mutants (30) to nearly 1/2 in an *exo1Δ* strain (31), to as little as ∼1/4 in an *sgs1Δ* mutant (14,25) along with a much greater decrease in repair by single-strand annealing of a DSB between flanking repeats. Most resection at a clean DSB was ascribed to Exo1 and Sgs1/Dna2 since there was almost no resection in the *sgs1Δ exo1Δ* double mutant.

Here, using the PFGE-shift approach, we examined the impact of the *exo1Δ* and *sgs1Δ* mutants on resection at a single random 'dirty' DSB created in circular ChrIII within a cellular milieu with many IR-DSBs across the genome. A break in the circular chromosome results in a unit length molecule. PFGE-shift can be detected with 15 min of radiation, which corresponds to resection of ∼200–400 nucleotides based on estimates from Westmoreland *et al.* (15). As shown in Figure 2, within 30 min following a dose of 20 krad, which produces around 40 DSBs per G2-cell, the length of resection in the single mutants appeared less than that of the WT cells. The disappearance of the linearized (broken) circle at later times due to repair/recircularization hindered further characterization. In order to prevent repair of the linearized/broken circles, we examined effects of Exo1 and Sgs1 on resection in a *rad51Δ* background. This approach allowed continued monitoring of resection up to 4 h after IR (Supplementary Figure S2 portrays enhanced detection of PFGE shift in *rad51Δ* at later times.) As described in Figure 3A, the resection in the double mutants was considerably reduced when compared with the *rad51Δ* single mutants at 20 krad.

In order to compare the relative effects of the *exo1Δ* and *sgs1Δ* deficiencies more precisely, the resection in each mutant following a 20 krad exposure was examined at identical times in adjacent lanes. As shown in Figure 3B, resection at IR-DSBs was clearly detected at 30 min, but was reduced by deletion of the *EXO1* or the *SGS1* genes. Based on our previous estimation of 1–2 kb per hour (15), the amount of resection after 30 min at the IR-DSB in the circular chromosome was about 500–1000 bases in the *rad51Δ* mutant. It appears that resection for either double mutant was about half the rate of that in the *rad51Δ* alone, based on the time required for comparable PFGE shifts.

Although the rate of resection in each of the double mutants (*exo1Δ rad51Δ* and *sgs1Δ rad51Δ*) is reduced compared to *rad51Δ*, there is rapid and comparable initiation of resection for both the mutants and the WT based on the loss of unresected linear molecules and the increased amount of PFGE-shifted DNAs at 30 min and 1 h. This pattern of PFGE-shift, where there is a single m** band that *moves up* the gel with time of incubation, indicates that resection is coordinated, unlike what is found for an *mre11-null* mutant, described in Figure 3C and in Westmoreland *et al.* (20), where there are only partially shifted molecules (m*) at early times indicative of one end resection and only a limited amount of fully shifted molecules (m**) at later times. (Resection is also coordinated in *rad51Δ* and *rad52Δ* mutants.) While there was a small reduction in resection in the *exo1Δ* and *sgs1Δ* cells, there was little if any effect on the kinetics of repair of multiple DSBs, as shown in Figure 3D. (Chromosomal repair was determined using the 'stained gel, multiple band method' described in (15) and here in the Materials and Methods.)

Previously, we had shown that in the absence of Mre11, initiation of resection at IR-DSB ends is severely reduced and mostly one-ended. While there is substantial resection in the *exo1Δ* and the *sgs1Δ* mutants, the limited resection at an IR-DSB in cells deficient in Mre11 is primarily due to Exo1 (Figure 3C). Comparable results are found in Supplementary Figure S3a and for the *rad50Δ* versus *rad50Δ exo1Δ* strains in Supplementary Figure S3b). This more severe defect in resection in the *exo1Δ mre11Δ* double mutant has little or no effect on IR survival (Figure 1).

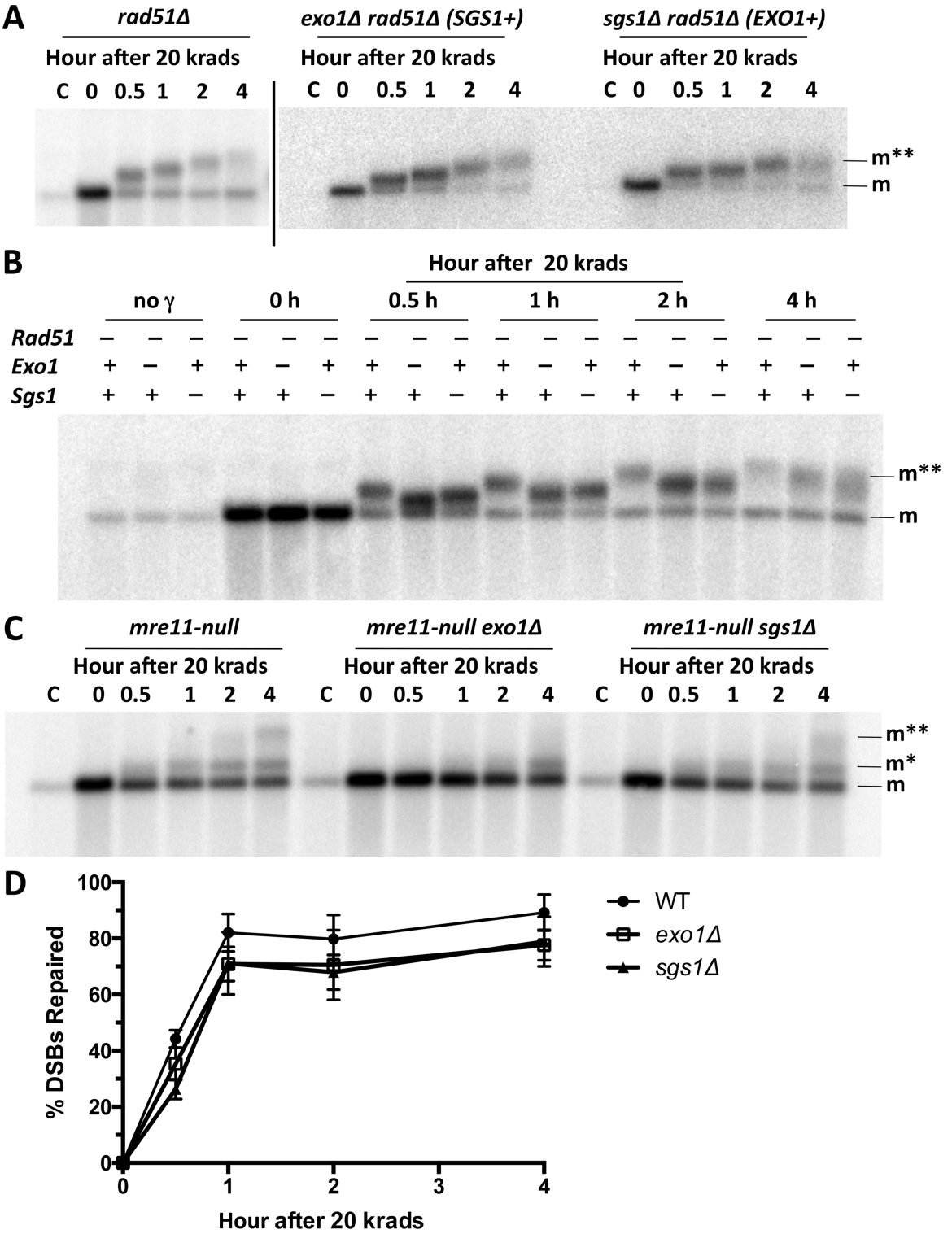

Figure 3. In absence of either Exo1 or Sgs1, the resection rate is reduced ∼50% while DSB repair kinetics in the single mutants is comparable to WT. (**A**) In the absence of Rad51, resection as indicated by PFGE-shift can be monitored during the entire post-IR incubation. The absence of either Exo1 or Sgs1 reduces the resection rate. (**B**) In this alternate gel loading format, side-by-side comparison of the three strains at each time point shows that Exo1 contributes more than Sgs1 to extensive resection in the first 30 min after 20 krads; however, by 1 h, the *exo1Δ rad51Δ* and *sgs1Δ rad51Δ* double mutant strains have almost equal PFGE-shift. The effects of Exo1 and Sgs1 appear to be additive, not synergistic, because the amount of shift in either double mutant at 1 h is similar to that of the *rad51Δ* single mutant at 0.5 h, and the amount at 2 h for the double mutants is comparable to the *rad51Δ* strain at 1 h. The overall rate of extensive resection in each of the double mutants is concluded to be about half that of the fully resection-proficient *rad51Δ* strain. (**C**) In the absence of MRX complex, most of the residual initiation of resection is carried out by Exo1. The PFGE-shift position of linearized ChrIII molecules resected at only one DSB end is indicated by 'm*.' (**D**) In spite of the ∼50% reduction in the rate of resection, loss of either Exo1 or Sgs1 has little or no effect on the DSB repair rate. Error bars are SEM and each data set is the mean of three experiments.

In *exo1Δ sgs1Δ* cells resection, but not recombinational repair, of IR-DSBs is greatly reduced

As described in Figure 4A, nearly all resection at an IR-DSB up to 4 h following a dose of 20 or 80 krad is due to the combination of Exo1 and SGS1/Dna2 based on PFGE shift analysis. This is consistent with reports that there is only a small amount of resection in *exo1Δ sgs1Δ* mutants at a single clean DSB and this is mediated by MRX and Sae2 (also using Southern analysis) (14,13). We found that there was no detectable PFGE-shift of the IR broken chromosome from the *exo1Δ sgs1Δ* strain when examined by Southern analysis. However, a small PFGE-shift could be detected on the original SybrGold-stained gels. As shown in Figure 4B, the band position of unbroken ChrVI molecules was visible just below the linearized ChrIII band and could be used as a reference for unresected/nonshifting DNA. During the time course, the position of the linearized ChrIII slowly shifted, reaching an apparent size increase of ∼20 kb at 4 h after 80 krads as described in Figure 4C. Importantly, at this level of detection nearly all the linearized molecules are shifted suggesting that all broken ends are subject to resection, albeit at a low rate. (See Supplementary Figure S4 for an additional example of this result.) Based on our previous estimates (15) and information in Figure 4C, the ∼20 kb pulse-field shift at 4 h corresponds to nearly 200–400 bases of resection at each end of the broken molecules. This amount of resection is around 10- to 20-fold less than for IR-DSBs in Exo1 Sgs1 proficient cells (i.e. cells with just a *rad51Δ* mutation).

Given the small amount of resection, we investigated its effect on the repair of IR-DSBs across the genome after exposing the G2 cells to 20 or 80 krad. As depicted in Figure 4D, after a dose of 20 krad, ∼30–40% and 60% of the DSBs were repaired at 1 and 2 h, respectively, in the *exo1Δ sgs1Δ* strain, as compared with >80% repair in the WT cells (the less than 100% is in part due to some cells in the population being in G1). Following a dose of 80 krad, where repair was ∼40% and 80% in the WT cells at 1 and 2 h, the corresponding values for the *exo1Δ sgs1Δ* strain are ∼20% and ∼55%, even though resection per end is estimated to be <100 bases and <200 bases at these times compared to 10- to 20-fold more resection in the $Exo^{+}Sgs1^{+}$ cells. Thus, the greatly reduced resection length in the *exo1Δ sgs1Δ* strain has only a modest effect on recombinational repair. This result for many IR-DSBs in G2 cells is comparable to previous studies examining the fate of a single HO-endonuclease induced DSB.

While the predominant mode of DSB repair in G2 cells is through recombination between sister chromatids, broken chromosomes could potentially be repaired by *de novo* telomere addition. Previously, telomere addition was shown to be a significant pathway for repair of HO-induced DSBs in the absence of Sgs1 and Exo1. (22,21). However, in these model systems there was no unbroken sister chromatid available for recombinational repair. In our system, repair of random IR-DSBs in the circular ChrIII by *de novo* telomere addition would be expected to result in stable, linearized chromosomes for those DSBs that occur at any position that is not within or near essential DNA. To address whether *de novo* telomere repair is a major repair pathway following IR in G2 arrested *exo1Δ sgs1Δ* cells, we examined 25 survivor colonies arising after 40 krad and 15 after 80 krad (corresponding to an estimated total of 80 DSBs among the 40 pairs of ChrIII chromatids) using PFGE analysis. Among the 40 colonies, there were no linear ChrIII molecules (an example of 10 colonies is presented in Supplementary Figure S5). The absence of stable linear ChrIII molecules, along with the result in Figure 4D that ∼70% to 80% of genome wide DSBs were conservatively repaired (i.e. the repair pathway(s) that were utilized gave rise to full-length, reconstituted chromosomes) during the 4 h time course, suggests that *de novo* telomere addition is not a major repair pathway for IR-DSBs in G2-arrested *exo1Δ sgs1Δ* cells. This is likely due to the availability of and preference for sister chromatid recombination in G2 arrested cells.

The lack of resection does not prevent crossing-over between ChrIII sister chromatids

We also examined the generation of recombinant ChrIII molecules. Previously, we found (15) that within 30 to 60 min. after IR exposure, the broken ChrIII chromosomes could generate dimer length molecules that were dependent upon Rad52, as also presented here in Figure 2 (d and d** after resection of the dimer). The resected and unresected dimer molecules that were attributed to crossing-over between sister chromatids (15) were also detected in the *exo1Δ* and *sgs1Δ* cells, similar to the WT. Importantly, we found that recombinants could be generated even in the absence of both genes. As shown in Figure 4A, there is a large increase in the amount of ChrIII dimers by 60 min after exposing the *exo1Δ sgs1Δ* cells to 80 krad. However, as for the case of linearized ChrIII unit length molecules, there is no detectable PFGE-shift. Since generation of the dimers depends on Rad51, these results are a direct demonstration that very little resection is required either for the recombinational repair of IR-DSBs between sister chromatids or for the generation of recombinant dimers.

DISCUSSION

There are two broad categories of DSB repair (in eukaryotes): endjoining and recombination. Recombinational repair includes conservative exchanges between sister chromatids or homologous chromosomes, such as gene conversion and crossing over, as well as nonconservative strand-annealing and break-induced replication (BIR, reviewed in (32,33)). As suggested for yeast and for mammalian cells (discussed in the Introduction), the processing of the ends can determine pathways toward endjoining versus recombination. In the absence of resection, repair is channeled toward the former, and resection provides substrate for recombinational repair as well as reduces possibilities for endjoining. The nature of the ends can be important determinants in opportunities for resection and recombination, and damaged ends need to be processed. In yeast, MRX- and Sae2-dependent resection of IR-damaged ends is highly efficient, and removal of the damage is likely an intrinsic aspect of the mechanism of the initiation step of resection (34). Specific enzymes such as tyrosyl-DNA phosphodiesterases 1 and 2 (TDP1 and TDP2), polynucleotide kinase phosphatase (PNK), aprataxin and the apurinic endonucleases

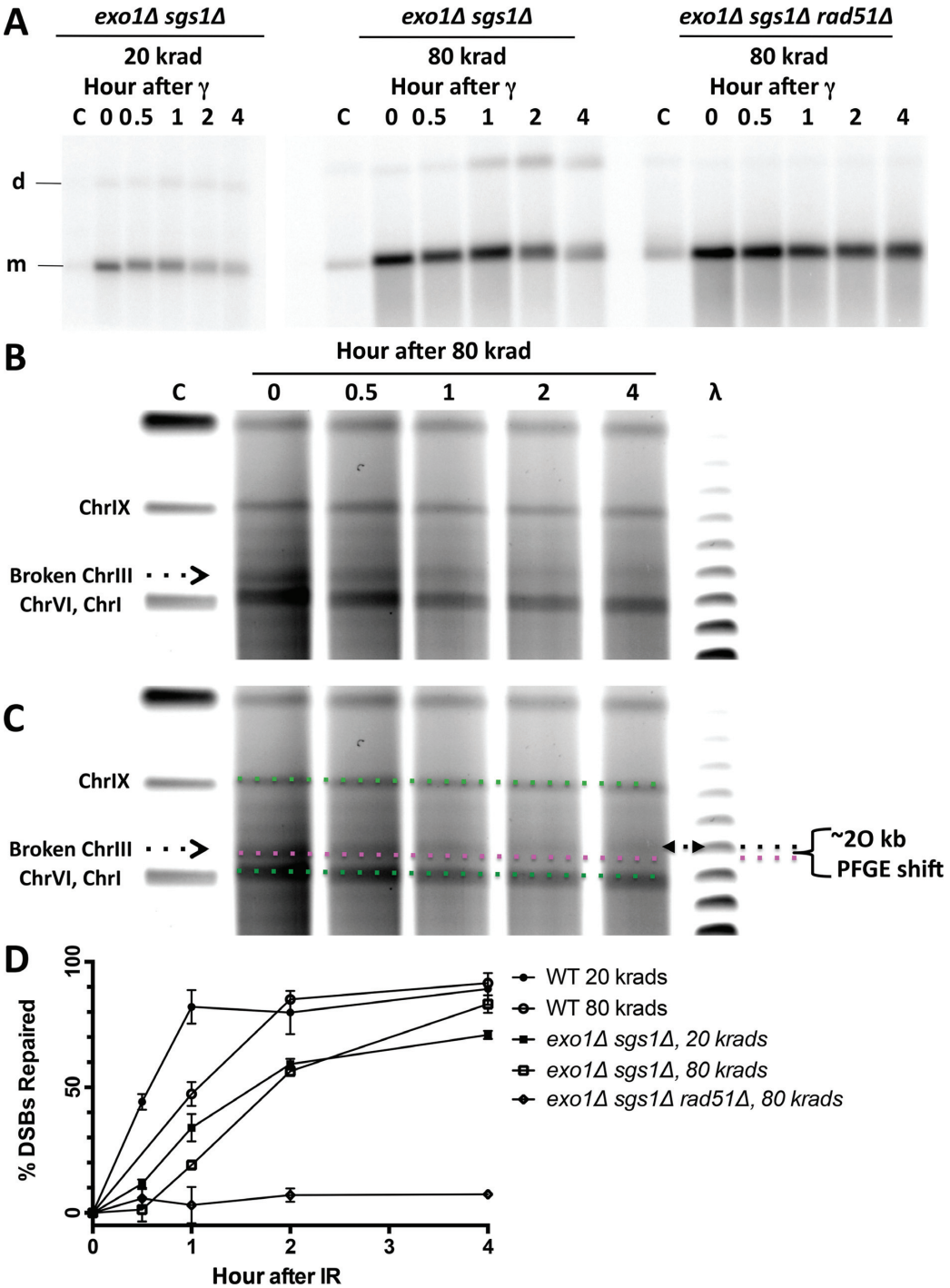

Figure 4. In the absence of both Sgs1 and Exo1, resection is greatly reduced after IR, but not survival or DSB repair. (**A**) PFGE-shift in *exo1Δ sgs1Δ* or *exo1Δ sgs1Δ rad51Δ* is barely detectable on Southerns using a ChrIII specific probe. In the *exo1Δ sgs1Δ* double mutant, dimer formation 'd' indicates that DSB recombinational repair can occur. (**B**) After 80 krads, some PFGE-shift is detectable in an *exo1Δ sgs1Δ rad51Δ* strain using SYBR® Gold-stained CHEF gels. The initial position of the broken Chr III is indicated by the dotted black arrow. With time, the distance between the ChrI/VI band and the linearized ChrIII increases due to PFGE-shift. (**C**) Using the image presented in 4B, the 'apparent' PFGE shift can be estimated. The parallel green dotted lines indicate the positions of the ChrI/VI and ChrIX bands. The ChrI/VI band provides a reference and compensates for unevenness in the electric field strength across the lanes during the PFGE run. The parallel magenta dotted line shows the initial position of the broken ChrIII and provides a reference for comparison with the final PFGE-shifted position 4 h after treatment with 80 krads. This final position is indicated by the black double-arrow. Comparison with the distance between Lambda ladder markers (48.5 kb between markers) indicates that the apparent shift is ∼20 kb at 4 h after IR treatment. By contrast, PFGE-shift in the resection proficient *rad51Δ* or WT cells results in an apparent increase in size of ∼20 kb and >40 kb at 15 and 30 min after 80 krad, respectively (estimated from (15); a similar result is found for 20 krad). Assuming an approximate constant rate of resection, this shift in the *rad51Δ* cells corresponds to a rate of resection of 0.25–0.5 kb per end at 15 min after 80 krad (0.5 to 1 kb per end at 30 min (15)). (**D**) Although DSB repair in *exo1Δ sgs1Δ* is delayed compared to WT (it takes two to three times as long to repair the first ∼40 to 50% of DSBs), by 4 h following 20 or 80 krads the repair of DSBs in *exo1Δ sgs1Δ* approaches that of WT, with 70 to 80% DSB repair in *exo1Δ sgs1Δ* versus ∼90% in WT cells. (20)

APE1 and APE2 can process damaged ends to prepare the DNA for repair (35,36).

Several factors have now been ascribed to determining the level and the rate of resection at clean DSB ends as well as the coordination. Previously, we showed a marked difference in processing clean versus dirty ends where Sae2 and Mre11 nuclease were required for efficient initiation and coordination of resection between IR-DSB ends, but not the ends of clean DSBs (20). The combination of Sae2 and MRX provides tethering opportunities for interactions between DSB ends. Sae2 appears to facilitate Mre11 nuclease positioning approximately 20 bases distant from the ends (37). The Ctp1 homolog from fission yeast has recently been shown to bridge ends of broken molecules (38). While Sae2 influences resection at DSB ends and coordination of resection at IR-DSBs, it does not appear to affect tethering based on results with unique probes near each end (39,40), although results with a single common probe suggest there may be a role in tethering (25,41). Once resection begins and RPA has coated the ssDNA, Rad52 and Rad51 provide for development of recombinational filaments. Also, Rad9 was recently found to not only attenuate extensive resection but also to enhance opportunities to load proteins associated with recombination (25).

Here, we establish in a population of ChrIII molecules with a single IR-DSB that extensive resection can be accomplished by either Exo1 or Sgs1/DNA2 alone, although the rate appears reduced by approximately half compared to WT suggesting that they act independently. However, global DSB repair in the single *exo1Δ* and *sgs1Δ* mutants is comparable to that in the WT, suggesting that even a 2-fold reduction in resection is tolerated well. This result with the *sgs1Δ* mutant differs from that of (42), who examined repair of a replication-associated DSB in a plasmid. They found that the rate of sister chromatid repair for replication derived DSBs in the plasmid based TINV system ((23) and see Introduction) was reduced by 50% compared to WT. Among the factors that might contribute to this difference are chromosomal versus plasmid location of the DSB, G2 versus replication-associated DSB and many radiation-induced DSBs versus a single DSB during replication. Also the systems are markedly different in their ability to detect recombinational repair. DSB repair in our system using PFGE is measured by the restoration of full-length linear chromosomes. This includes allelic gene conversion and crossing over. In the plasmid based system, which registers recombination between allelic or nonallelic repeats, allelic gene conversion is not detected even though this is likely the major source of repair between chromosomal sister chromatids.

In the absence of MRX, Exo1 has a greater role in resection at dirty DSBs than Sgs1/DNA2 (Figure 3C and Supplementary Figure S2). In the absence of both Exo1 and Sgs1, resection is extremely slow with a rate corresponding at most to just a few bases per minute. The remaining resection at the IR-DSBs is likely due to MRX and Sae2 (20). Regardless, we observed considerable repair in the *exo1Δ sgs1Δ* strain, where it only took an additional hour over the WT or the single mutants to repair ∼50% of the DSBs across the genome. While survival was decreased it was still much higher than for *mre11Δ* or *rad51Δ* mutants. Since there was no difference in survival between G-2 irradiated *exo1Δ sgs1Δ* and *exo1Δ sgs1Δ dnl4* cells, we conclude that the repair under conditions of little resection is not due to endjoining.

These findings lead us to conclude that recombinational repair of multiple IR-DSBs can occur without extensive resection, i.e. without Exo1 and Sgs1/Dna2. This result is consistent with the impact of the *exo1Δ sgs1Δ* defect on sister chromatid repair of the TINV plasmid based replication-associated DSB (42), although there was no direct measurement of resection and the repair products detected (nonallelic recombinant molecules) differed from those in the present system (restitution of full length chromosomes). Furthermore, we provide the first direct molecular demonstration that there is at most a need for only limited resection in the induction of recombined sister chromatid molecules by IR-DSBs, based on the appearance of ChrIII dimers within 1 h after irradiation (Figure 4A) in spite of a severe reduction in resection length. Earlier studies addressing heteroallelic recombination with a defined DSB also indicated that extensive resection might not be needed. Although several kb of resection were suggested based on preferential recombination at sites distant from the break (43), strand invasion DNA synthesis associated with Mat switching and product formation could be observed as early as 60 min following HO-break induction (44,45). Furthermore, it was reported that a four-fold reduction in resection rate due to loss of the FUN30 chromatin remodeling gene does not decrease gene conversion induced by a site-specific DSB (30,46). Based on analysis of DSB associated recombinants, gene conversion can involve stretches in the range of hundreds of bases (47).

In the original model for recombinational repair of DSBs (6), resection was invoked to create a recombinational 3′ single-strand that could associate with DNA of an unbroken chromosome in order to copy information across the break. This is formally equivalent to models of DSB-associated recombination described much later (summarized in (8)). Since in yeast systems, recombination requires Rad52 to replace RPA on resected DNA and the subsequent generation of Rad51 filaments (48), the present results demonstrate that the initiation of recombination and completion of repair of IR-DSBs in cells with many DSBs can occur with very short filaments.

Although there is regulation of extensive resection in yeast by Rad9 (25), at least for the case of a unique single DSB, the question remains about the purpose of the observed excess in resection. Even in WT cells, there are approximately 500–1000 bases removed per DSB end within 30 min after a dose of 20 krad, by which time 40% of the nearly 40 breaks/cells are repaired. Possibly the excess resection provides signaling associated with ssDNA or generation of an enlarged pool of nucleotides that could be used in the process of repair replication across a break.

Regions in the vicinity of DSBs are highly mutation prone to either spontaneous or induced lesions, and hypermutability was attributed to the appearance of long resected regions, which would not be subject to template-dependent excision repair (49,50). Resection length before completed DSB repair could determine the potential for such mutagenesis. Possibly, reduction in resection as described here

would reduce the likelihood of this DSB-associated localized hypermutability. Interestingly, using a similar PFGE assay system based on changes in the circular ∼175 kb EBV, it appears there is little resection in human cells following IR exposure (11) even when endjoining is inhibited.

The large amount of resection seen in WT cells during recombinational repair of IR-DSBs could also assure checkpoint signalling that would prevent division prior to repair. However, in the present studies this is not relevant since cells are arrested in G2 and held in nocodazole during the 4 h repair period. It is interesting to consider the impact of short and long regions of resection on recombination opportunities. Our results demonstrate that recombinational repair of multiple 'dirty' IR-DSBs can be efficient under conditions of short resection. If regions of resection are short, then opportunities for single-strand annealing interactions must be greatly reduced. It is also possible that longer stretches of resection might assure longer regions of interaction, i.e. between sister chromatids or homologous chromosomes, to avoid aberrant ectopic recombinational events (22) as occasionally found for IR-DSBs (29). Previously, we showed that under conditions of decreased cohesin the strong preference for sister chromatid recombination in the repair of IR-DSBs is greatly relaxed, resulting in large increases in recombination between homologs (18). Interestingly, the rate of IR-DSB repair is reduced under those conditions as compared to repair of DSBs between sister chromatids. Given the greater time required for the repair, much more resection would be anticipated. This enhanced resection might increase the likelihood of repair between the homologs because of the larger DNA regions or filaments available in the search for homology.

It is important to note that, except for the plasmid based TINV assay developed in the Aguilera lab (23), questions of allelic recombination between sister chromatids versus global recombination between homologous chromosomes or regions of homology across the genome can only be addressed by examining random breaks. Unlike for enzymes such as HO-endonuclease, DSBs would only rarely appear at or near the same site in sister chromatids. It would be interesting in future studies to pursue further the relationship between resection at IR-DSBs and global recombination by reducing resection using the single *exo1Δ* and *sgs1Δ* or the double mutants. Similarly, it would be interesting to look at homology-dependent IR-induced chromosomal rearrangements between small repeats across the genome, which were found to be substantial in irradiated diploid WT cells that were in G2 (29). Many of those rearrangements were considered to arise through BIR. In the present experiments involving G2 haploid cells, conservative BIR between sister chromatids would yield full length, reconstituted chromosomes and thus be indistinguishable from either gene conversion or crossover recombination in our DSB repair assay. However, BIR appears to be a slow process (51), unlike the DSB repair that occurs within 1 to 2 h in the present study. Finally, since human cells contain homologs of Exo1 and Dna2 as well as the RecQ proteins BLM and WRN that function like Sgs1 with DNA2 toward clean breaks (52), the present findings are expected to enhance our understanding of how these human related proteins might respond toward IR-DSBs.

SUPPLEMENTARY DATA

Supplementary Data are available at NAR Online.

ACKNOWLEDGEMENT

We thank members of the Resnick Lab for many useful discussions and to Drs Sara Andres and Kin Chan for critical reading of the manuscript and suggestions.

FUNDING

Intramural Research Program of the National Institute of Environmental Health Sciences (National Institutes of Health, Department of Health and Human Services) [Project 1 Z01 ES065073 to M.A.R.]. Funding for open access charge: NIH in-house funds.
Conflict of interest statement. None declared.

REFERENCES

1. Ward,J.F. (1994) The complexity of DNA damage: relevance to biological consequences. *Int. J. Radiat. Biol.*, **66**, 427–432.
2. Goodhead,D.T. (1994) Initial events in the cellular effects of ionizing radiations: clustered damage in DNA. *Int. J. Radiat. Biol.*, **65**, 7–17.
3. Westmoreland,J.W., Summers,J.A., Holland,C.L., Resnick,M.A. and Lewis,L.K. (2010) Blunt-ended DNA double-strand breaks induced by endonucleases PvuII and EcoRV are poor substrates for repair in Saccharomyces cerevisiae. *DNA Rep.*, **9**, 617–626.
4. Granata,M., Panigada,D., Galati,E., Lazzaro,F., Pellicioli,A., Plevani,P. and Muzi-Falconi,M. (2013) To trim or not to trim: progression and control of DSB end resection. *Cell cycle*, **12**, 1848–1860.
5. Chapman,J.R., Taylor,M.R. and Boulton,S.J. (2012) Playing the end game: DNA double-strand break repair pathway choice. *Mol. Cell*, **47**, 497–510.
6. Resnick,M.A. (1976) The repair of double-strand breaks in DNA; a model involving recombination. *J. Theor. Biol.*, **59**, 97–106.
7. Szostak,J.W., Orr-Weaver,T.L., Rothstein,R.J. and Stahl,F.W. (1983) The double-strand-break repair model for recombination. *Cell*, **33**, 25–35.
8. Haber,J.E. (2008) Evolution of models of homologous recombination. *Genome Dyn. Stab.*, **3**, 1–64.
9. Daley,J.M. and Sung,P. (2014) 53BP1, BRCA1, and the choice between recombination and end joining at DNA double-strand breaks. *Mol. Cell. Biol.*, **34**, 1380–1388.
10. Di Virgilio,M., Callen,E., Yamane,A., Zhang,W., Jankovic,M., Gitlin,A.D., Feldhahn,N., Resch,W., Oliveira,T.Y., Chait,B.T. *et al.* (2013) Rif1 prevents resection of DNA breaks and promotes immunoglobulin class switching. *Science*, **339**, 711–715.
11. Ma,W., Halweg,C.J., Menendez,D. and Resnick,M.A. (2012) Differential effects of PARP inhibition and depletion on single- and double-strand break repair in human cells are revealed by changes in EBV minichromosomes. *Proc. Natl. Acad. Sci. U.S.A.*, **109**, 6590–6595.
12. Mimitou,E.P. and Symington,L.S. (2011) DNA end resection–unraveling the tail. *DNA Rep.*, **10**, 344–348.
13. Mimitou,E.P. and Symington,L.S. (2008) Sae2, Exo1 and Sgs1 collaborate in DNA double-strand break processing. *Nature*, **455**, 770–774.
14. Zhu,Z., Chung,W.-H., Shim,E.Y., Lee,S.E. and Ira,G. (2008) Sgs1 helicase and two nucleases Dna2 and Exo1 resect DNA double-strand break ends. *Cell*, **134**, 981–994.
15. Westmoreland,J., Ma,W., Yan,Y., Van Hulle,K., Malkova,A. and Resnick,M.A. (2009) RAD50 is required for efficient initiation of resection and recombinational repair at random, gamma-induced double-strand break ends. *PLoS Genet.*, **5**, e1000656.
16. Ma,W., Westmoreland,J., Nakai,W., Malkova,A. and Resnick,M.A. (2011) Characterizing resection at random and unique chromosome double-strand breaks and telomere ends. *Methods Mol. Biol.*, **745**, 15–31.

17. Game,J.C., Sitney,K.C., Cook,V.E. and Mortimer,R.K. (1989) Use of a ring chromosome and pulsed-field gels to study interhomolog recombination, double-strand DNA breaks and sister-chromatid exchange in yeast. *Genetics*, **123**, 695–713.
18. Covo,S., Westmoreland,J.W., Gordenin,D.A. and Resnick,M.A. (2010) Cohesin Is limiting for the suppression of DNA damage-induced recombination between homologous chromosomes. *PLoS Genet.*, **6**, e1001006.
19. Ma,W., Westmoreland,J.W., Gordenin,D.A. and Resnick,M.A. (2011) Alkylation base damage is converted into repairable double-strand breaks and complex intermediates in G2 cells lacking AP endonuclease. *PLoS Genet.*, **7**, e1002059.
20. Westmoreland,J.W. and Resnick,M.A. (2013) Coincident resection at both ends of random, gamma-induced double-strand breaks requires MRX (MRN), Sae2 (Ctp1), and Mre11-nuclease. *PLoS Genet.*, **9**, e1003420.
21. Lydeard,J.R., Lipkin-Moore,Z., Jain,S., Eapen,V.V. and Haber,J.E. (2010) Sgs1 and exo1 redundantly inhibit break-induced replication and de novo telomere addition at broken chromosome ends. *PLoS Genet.*, **6**, e1000973.
22. Chung,W.H., Zhu,Z., Papusha,A., Malkova,A. and Ira,G. (2010) Defective resection at DNA double-strand breaks leads to de novo telomere formation and enhances gene targeting. *PLoS Genet.*, **6**, e1000948.
23. Gonzalez-Barrera,S., Cortes-Ledesma,F., Wellinger,R.E. and Aguilera,A. (2003) Equal sister chromatid exchange is a major mechanism of double-strand break repair in yeast. *Mol. Cell*, **11**, 1661–1671.
24. Ira,G., Pellicioli,A., Balijja,A., Wang,X., Fiorani,S., Carotenuto,W., Liberi,G., Bressan,D., Wan,L., Hollingsworth,N.M. *et al.* (2004) DNA end resection, homologous recombination and DNA damage checkpoint activation require CDK1. *Nature*, **431**, 1011–1017.
25. Ferrari,M., Dibitetto,D., De Gregorio,G., Eapen,V.V., Rawal,C.C., Lazzaro,F., Tsabar,M., Marini,F., Haber,J.E. and Pellicioli,A. (2015) Functional interplay between the 53BP1-Ortholog Rad9 and the Mre11 complex regulates resection, end-tethering and repair of a double-strand break. *PLoS Genet.*, **11**, e1004928.
26. Ma,W., Resnick,M.A. and Gordenin,D.A. (2008) Apn1 and Apn2 endonucleases prevent accumulation of repair-associated DNA breaks in budding yeast as revealed by direct chromosomal analysis. *Nucleic Acids Res.*, **36**, 1836–1846.
27. Goldstein,A.L. and McCusker,J.H. (1999) Three new dominant drug resistance cassettes for gene disruption in Saccharomyces cerevisiae. *Yeast*, **15**, 1541–1553.
28. Storici,F., Lewis,L.K. and Resnick,M.A. (2001) In vivo site-directed mutagenesis using oligonucleotides. *Nat. Biotechnol.*, **19**, 773–776.
29. Argueso,J.L., Westmoreland,J., Mieczkowski,P.A., Gawel,M., Petes,T.D. and Resnick,M.A. (2008) Double-strand breaks associated with repetitive DNA can reshape the genome. *Proc. Natl. Acad. Sci. U.S.A.*, **105**, 11845–11850.
30. Eapen,V.V., Sugawara,N., Tsabar,M., Wu,W.H. and Haber,J.E. (2012) The Saccharomyces cerevisiae chromatin remodeler Fun30 regulates DNA end resection and checkpoint deactivation. *Mol. Cell. Biol.*, **32**, 4727–4740.
31. Chen,H., Lisby,M. and Symington,L.S. (2013) RPA coordinates DNA end resection and prevents formation of DNA hairpins. *Mol. Cell*, **50**, 589–600.
32. Anand,R.P., Lovett,S.T. and Haber,J.E. (2013) Break-induced DNA replication. *Cold Spring Harbor Perspect. Biol.*, **5**, a010397.
33. Malkova,A. and Ira,G. (2013) Break-induced replication: functions and molecular mechanism. *Curr. Opin. Genet. Dev.*, **23**, 271–279.
34. Garcia,V., Phelps,S.E., Gray,S. and Neale,M.J. (2011) Bidirectional resection of DNA double-strand breaks by Mre11 and Exo1. *Nature*, **479**, 241–244.
35. Andres,S.N., Schellenberg,M.J., Wallace,B.D., Tumbale,P. and Williams,R.S. (2015) Recognition and repair of chemically heterogeneous structures at DNA ends. *Environ. Mol. Mutagen.*, **56**, 1–21.
36. Povirk,L.F. (2012) Processing of damaged DNA ends for double-strand break repair in mammalian cells. *ISRN Mol. Biol.*, **2012**, doi:10.5402/2012/345805.
37. Cannavo,E. and Cejka,P. (2014) Sae2 promotes dsDNA endonuclease activity within Mre11-Rad50-Xrs2 to resect DNA breaks. *Nature*, **514**, 122–125.
38. Andres,S.N., Appel,C.D., Westmoreland,J.W., Williams,J.S., Nguyen,Y., Robertson,P.D., Resnick,M.A. and Williams,R.S. (2015) Tetrameric Ctp1 coordinates DNA binding and DNA bridging in DNA double-strand-break repair. *Nat. Struct. Mol. Biol.*, **22**, 158–166.
39. Lobachev,K., Vitriol,E., Stemple,J., Resnick,M.A. and Bloom,K. (2004) Chromosome fragmentation after induction of a double-strand break is an active process prevented by the RMX repair complex. *Curr. Biol.*, **14**, 2107–2112.
40. Nakai,W., Westmoreland,J., Yeh,E., Bloom,K. and Resnick,M.A. (2011) Chromosome integrity at a double-strand break requires exonuclease 1 and MRX. *DNA Rep.*, **10**, 102–110.
41. Clerici,M., Mantiero,D., Lucchini,G. and Longhese,M.P. (2005) The Saccharomyces cerevisiae Sae2 protein promotes resection and bridging of double strand break ends. *J. Biol. Chem.*, **280**, 38631–38638.
42. Munoz-Galvan,S., Lopez-Saavedra,A., Jackson,S.P., Huertas,P., Cortes-Ledesma,F. and Aguilera,A. (2013) Competing roles of DNA end resection and non-homologous end joining functions in the repair of replication-born double-strand breaks by sister-chromatid recombination. *Nucleic Acids Res.*, **41**, 1669–1683.
43. Inbar,O. and Kupiec,M. (1999) Homology search and choice of homologous partner during mitotic recombination. *Mol. Cell. Biol.*, **19**, 4134–4142.
44. White,C.I. and Haber,J.E. (1990) Intermediates of recombination during mating type switching in Saccharomyces cerevisiae. *EMBO J.*, **9**, 663–673.
45. Hicks,W.M., Yamaguchi,M. and Haber,J.E. (2011) Real-time analysis of double-strand DNA break repair by homologous recombination. *Proc. Natl. Acad. Sci. U.S.A.*, **108**, 3108–3115.
46. Chen,X., Cui,D., Papusha,A., Zhang,X., Chu,C.D., Tang,J., Chen,K., Pan,X. and Ira,G. (2012) The Fun30 nucleosome remodeller promotes resection of DNA double-strand break ends. *Nature*, **489**, 576–580.
47. Sweetser,D.B., Hough,H., Whelden,J.F., Arbuckle,M. and Nickoloff,J.A. (1994) Fine-resolution mapping of spontaneous and double-strand break-induced gene conversion tracts in Saccharomyces cerevisiae reveals reversible mitotic conversion polarity. *Mol. Cell. Biol.*, **14**, 3863–3875.
48. San Filippo,J., Sung,P. and Klein,H. (2008) Mechanism of eukaryotic homologous recombination. *Annu. Rev. Biochem.*, **77**, 229–257.
49. Yang,Y., Sterling,J., Storici,F., Resnick,M.A. and Gordenin,D.A. (2008) Hypermutability of damaged single-strand DNA formed at double-strand breaks and uncapped telomeres in yeast Saccharomyces cerevisiae. *PLoS Genet.*, **4**, e1000264.
50. Chan,K., Sterling,J.F., Roberts,S.A., Bhagwat,A.S., Resnick,M.A. and Gordenin,D.A. (2012) Base damage within single-strand DNA underlies in vivo hypermutability induced by a ubiquitous environmental agent. *PLoS Genet.*, **8**, e1003149.
51. Malkova,A., Naylor,M.L., Yamaguchi,M., Ira,G. and Haber,J.E. (2005) RAD51-dependent break-induced replication differs in kinetics and checkpoint responses from RAD51-mediated gene conversion. *Mol. Cell. Biol.*, **25**, 933–944.
52. Sturzenegger,A., Burdova,K., Kanagaraj,R., Levikova,M., Pinto,C., Cejka,P. and Janscak,P. (2014) DNA2 cooperates with the WRN and BLM RecQ helicases to mediate long-range DNA end resection in human cells. *J. Biol. Chem.*, **289**, 27314–27326.